International Journal of Scientific Research in Engineering and Management (IJSREM)
Volume: 09 Issue: 08 | Aug - 2025 SJIF Rating: 8.586 ISSN: 2582-3930

Solar PV And Grid-Based Isolated Converter Utilizing Dual Sources to Charge Plug-In Electric Vehicles.

Author 1 Mr. Pradip Ramdas Jadhav

PG Scholar Mss'scet Jalna
Author 2 Prof Mr. K .Chandra Obula Reddy
Assistant Professor
Mss'scet ,Jalna
[1] pradipjadhav76652@gmail.com
2 chandra6279@gmail.com

Abstract— In this paper a multipurpose power electronic interface (PEI) competent of utilising dual sources during charging process has been proposed for plug-in electric vehicles. Based on the requirement, the battery can either be charged from solar photovoltaic (SPV) or from the grid. Moreover, when charged from an SPV source, converter can extract highest available power with maximum power point tracking (MPPT). The intrinsic novelty of the proposed PEI is that no additional components/switches are employed to achieve dual sources in charging or for MPPT. The proposed PEI consists of a converter derived from a conventional isolated secondary ended primary inductance converter (SEPIC). It is designed to operate effectively in all vehicular modes (charging, propulsion (PP) and regenerative braking (RB)). During battery charging from the grid and SPV, it operates as isolated SEPIC. While, in PP and RB, it operates as a fly back converter. Therefore, the proposed converter keeps isolation in each mode, which results in better safety for battery as well as vehicle users. Further, all vehicular modes are achieved through a single converter. As a result, compactness of the charger increases and making it best solution for on-board battery charging application.

I.INTRODUCTION

The continuous depletion of fossil fuels and increasing environmental issues led to research in pollution-free electric vehicles (EVs) or plug-in EVs (PEVs) across the world. The main components of an EV are charging system, battery management system (BMS) and inverter drive system. For full commercialization of EVs in market, the battery charging mechanism and development of battery technology are still challenges for vehicle manufacturers. Usually, the battery chargers are classified as on-board charger (OBC) and off-board charger. The OBC is more prevalent in EVs or PEVs because vehicle can be charged anywhere [1–3]. However, the OBC has constrained of the size and space because it is placed in the vehicle premises.

Depending on the number of stages aforementioned chargers can be further classified as; single-stage charger or two-stage charger. However, due to a large number of components in the two-stage charger [4–7], a single-stage charger is more attractive for on-board applications. Conventional single-stage conversion systems utilising grid and solar photovoltaic (SPV) are shown in

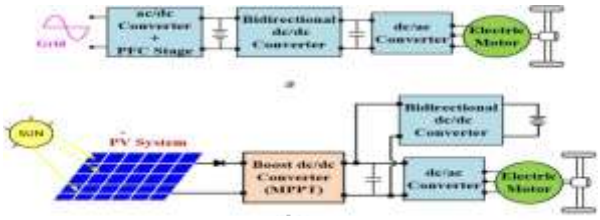

Fig. 1 *Block diagram of chargers*

(a)Conventional single-stage plug-in charger, ***(b)*** Conventional SPV system for a battery charger

(a) Figs. 1*a* and *b*, respectively. As it can be observed, even single-stage chargers utilise at least three converters for battery charging and discharging. To further reduce the number of components in single-stage charger researchers have proposed integrated chargers [8–18], which employs a fewer number of components compared to conventional single-stage charger. These integrated chargers are of two types. In the first type of integrated charger, bidirectional dc/dc converter connected between battery and dc link is integrated with charging circuit and in the second type of integrated charger, electric motor winding and traction converter are used in the charging circuit by employing some relays and mechanical switches, thereby eliminating additional inductor requirements for charging operation. This reduces the weight of charger because inductor is the heaviest component in converter compared to other components such as switch, diode and capacitor. Usually, these chargers operate in boost mode; therefore, to provide adequate voltage and current to the battery some manufacturers deploy a bidirectional dc/dc converter between dc link and the battery, which increases weight and cost to

the charging system. Further, these chargers have one or more following disadvantages: (i) specially designed windings; (ii) applicability to a certain type of electric machines; (iii) difficulty in accessing the neutral point of windings; (iv) reduced reliability due to mechanical contacts andcontrol complexity and extra hardware pose challenges in commercialisation; (vi) usually, operate in boost mode only. Integrated converters minimise the weight, size and cost of the chargers, and therefore they are advantageous, as the OBC is always carried on the vehicle. Most of the integrated chargers utilise non-isolated converter to achieve all modes of vehicular operation. Galvanic isolation is normally avoided in OBC because it has a negative effect on cost, weight, and sizing of the charger. Nevertheless, isolation is a very favourable option in the charger circuit to provide the safety for vehicle users and charger circuit. It also increases the battery life remarkably. Further, in mentioned integrated chargers, the battery is charged through the grid supply or regenerative braking (RB). The chargers in [19, 20] use only SPV system for battery charging. Usually, the battery charging from solar uses two converters (Fig. 1*b*); one for

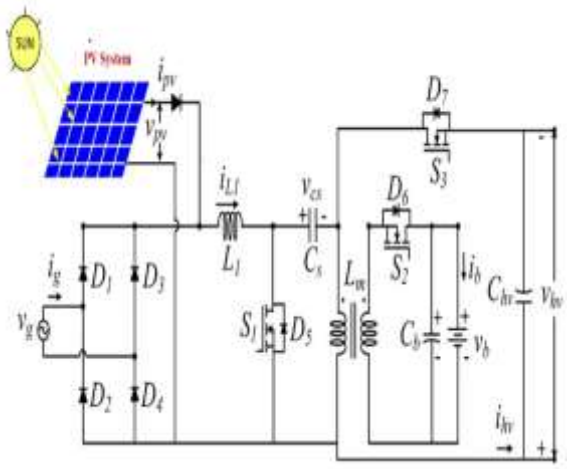

Fig. 2 *Structure of proposed power electronics interface (PEI)*

Table 1 States of semiconductor devices in each mode

Mode of operation	Figure	S_1	S_2	S_3	D_5	D_6	D_7
PIC and solar charging	Figs. 3a and 4	PWM	OFF	OFF	OFF	OFF	OFF
	Figs. 3b and 4	OFF	OFF	OFF	OFF	ON	OFF
PP	Fig. 5a	OFF	PWM	OFF	OFF	OFF	ON
RB	Fig. 5b	OFF	OFF	PWM	OFF	ON	OFF

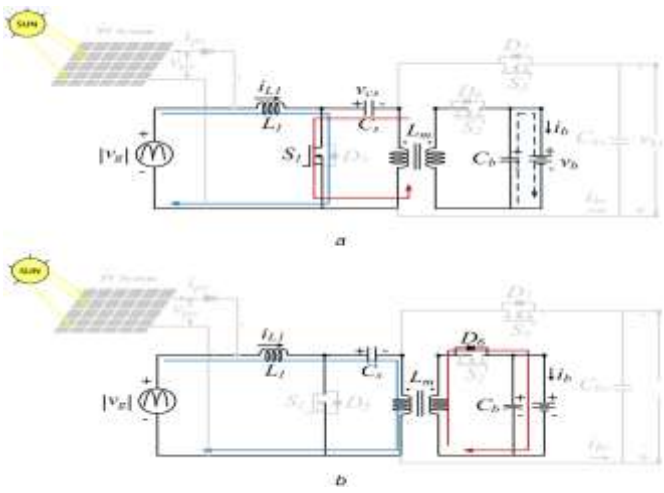

Fig. 3 Operation of the converter during PIC mode (a) Switch S1 is ON, (b) Switch S1 is OFF

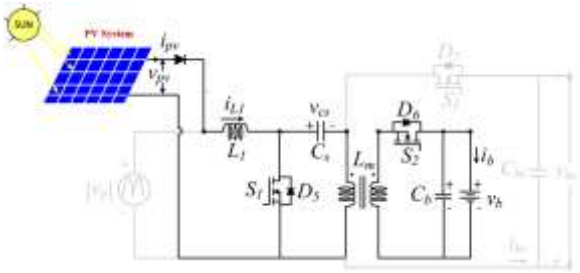

Fig. 4 Circuit representation for solar battery charging

maximum power point tracking (MPPT) and second bidirectional dc/dc converter maintains dc-link voltage controlled charging for the battery. It is concluded that in the reported integrated chargers, there is no such charger available, which provides galvanic isolation for all modes of vehicles as well as a supplementary renewable source (such as SPV) for the battery charging. In the context of the above literature review, this paper proposes a new grid and SPV-based integrated charger using galvanic

isolation, as shown in Fig. 2. The proposed converter is derived

from the conventional isolated secondary ended primary inductance converter (SEPIC), which operates as a SEPIC during battery charging from the grid and SPV and as a fly back converter during PP and RB modes. The main features of the grid and SPV based integrated charger compared to existing integrated chargers are as follows: (a) galvanic isolation in all vehicular modes, which results in better safety for battery and vehicle users. (b) plug-in and SPV charging is achieved with same converter (no additional converter is required for MPPT operation), (c) cost of fossil fuel based electricity reduces due to the SPV charging and (d) reliability of the charger increases due to dual sources for charging. In addition to this, proposed converter has buck/boost operation in all modes, which is desirable for vehicle application [21]. Due to buck/boost operation, a wide range of battery voltage can be

selected as well as the battery can be charged with a universal input voltage range 90–260 V. If PP machine operates with a

minimum voltage close to battery voltage, a dc/dc converter with a buck/
boost capability is preferred because battery voltage varies significantly depending on the state-of-charge (SOC). The remaining part of this paper is organized as follows: Section 2 discusses the converter operation all vehicular modes. Section 3 discusses the design of the proposed system. In Section 4, the loss analysis of the converter in each mode is discussed. Section 5 discusses the component lifetime. A comparative analysis of the proposed converter with existing integrated converters has been investigated in Section 6.

The control algorithms for different modes are discussed in Section 7. In Section 8, simulation and experimental results have been discussed to verify the proposed scenario. Finally, concluding remarks drawn from the simulation are given in Section 9.

2 Operation of the converter

Operation of the converter in SEPIC and fly back modes is discussed in the following sections. Moreover, operating states of switches and body diodes are given in Table 1.

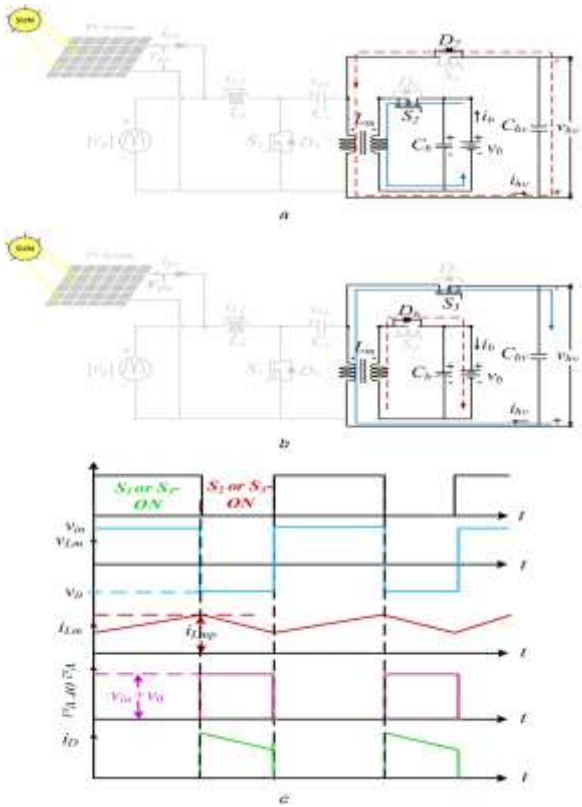

Fig. 5 Operation of the converter in (a) PP mode, (b) RB mode and, (c) Operation waveforms of PP and RB modes

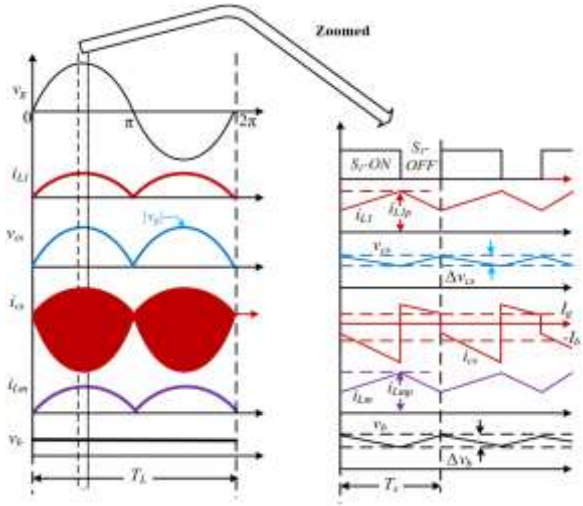

Fig. 6 Operation wave forms during line and switching cycles

2.1 Simulink mode of operation

In SEPIC mode of operation, the battery is charged through the grid as well as SPV system. When the battery is charged through
the grid, the operation mode is known as plug-in charging (PIC). 2.1.1 PIC mode: In this mode, SPV system will be deactivated and the battery is charged from the grid. When the switch S1 turns ON current through the inductor L1 follows the path as indicated by the blue line as shown in Fig. 3a. The electrostatic energy of capacitor Cs transformed into magnetic energy and stored in magnetising inductance (Lm) of high-frequency transformer (HFT) through the path as indicated by the red line. Meanwhile, a capacitor Cb connected at the battery terminal provides energy to the battery. When S1 turns OFF stored magnetic energy of Lm transfers to the output battery load as indicated by the red lines as shown in Fig. 3b. Further, during this mode, the capacitor Chv is charged up to peak grid voltage through the body diode D7 of the switch S3 and then D7 remains OFF throughout this mode. The operation wave forms of this mode during a line and switching cycles are shown in Fig. 6. 2.1.2 SPV mode: In this mode, the grid will be deactivated, and the battery is charged through SPV system. The output of solar is fed to the isolated SEPIC, and MPPT is performed using Equivalent circuit of this mode is shown in Fig. 4. The operation of converter in this mode is exactly the same as the converter operation in PIC.

2.2 Fly-back operation

During PP and RB modes, the proposed converter operates as a conventional fly back converter. In the following sections, the operation of both the modes is discussed with relevant wave forms (Fig. 5c). In Fig. 5c, vin and v0 are the input and output voltages, respectively, of PP and RB modes. While iD is the current through the diode D7 in PP mode D6 in RB mode. Moreover, iLm is the current through the magnetising inductance Lm in PP and RB modes. 2.2.1 PP mode: In PP mode, when the switch S2 turns ON, the magnetising inductance Lm of HFT stores energy and current through Lm

is indicated by the solid blue line, as shown in Fig. 5a. When S2 turns OFF inductor Lm transfers its stored energy to the dc-link capacitor Chv through the path as indicated by the red dotted line in Fig. 5a. 2.2.2 RB mode: The operation of regeneration (Fig. 5b) is exactly the same as PP mode in the reverse direction. In this mode, switch S3 turns ON, inductor Lm stores energy and the flow current through it is shown through the blue solid line. When S3 turns OFF, inductor Lm transfers its stored energy to the battery and its state of- charge (SOC) builds up. Control algorithms The control structure of the proposed PEI for all modes has been shown in Fig. 7. 7.1 PIC mode

In PIC mode, a two-loop proportional–integral (PI) controller Gib(z) is used to charge the battery. The outer loop is a power controller, which generates a reference signal for the inner PI controller GiL(z). The output of inner controller is compared with carrier signal to generate pulse-width modulation (PWM) signal for switch S1. 7.2 SPV mode The battery charging from SPV system is achieved through this converter for MPPT. The PWM signal from the MPPT controller is given to switch S1. The MPPT control block ensures maximum power point (MPP) operation for PV system by generating the duty cycle for isolated SEPIC. There are various MPPT techniques available in the literature to achieve MPP operation and any of them can be used However, perturb and observe (P&O) algorithm is widely used in a practical system due to its easy software and hardware implementation

The focus of this paper is not related to the MPPT algorithm, however, for completeness of the system, P&O-based MPPT is discussed in brief, which is explained in the following paragraph. The P&O method for MPPT is implemented by deliberately perturbing PV array output voltage and hence PV power output. The controller analyses these perturbed parameters before and after perturbation to arrive at MPP. The main equations of P&O method are described as

$D(k) = D(k-1) - \Delta D$, if $dppv \cdot dvpv > 0$ (8)

$D(k) = D(k-1) + \Delta D$, if $dppv \cdot dvpv < 0$ (9)

where ΔD is the perturb duty ratio. Fig. 8 shows a detail flowchart P&O MPPT algorithm. 7.3 PP and RB modes

The control block diagram for PP and RB modes has been shown in Fig. 7, which is closed with red dotted lines. In both the modes, the two-loop PI controller is used to give the PWM pulses for switches S2 and S3. Moreover, the inner PI controller is used for both the modes. The control targets of PP mode are to fix the dclink voltage at reference valued for smooth operation of vehicle.

The reference dc-link voltage is compared with measured dc-link voltage and error is supplied to the outer PI controller, which generates a reference signal for the inner PI controller. The output of the inner PI controller is compared to a triangular wave and generates PWM pulses for switch S2. In RB mode, usually, the input reference quantity can be torque or speed, which is determined by the driver [21]. The error between

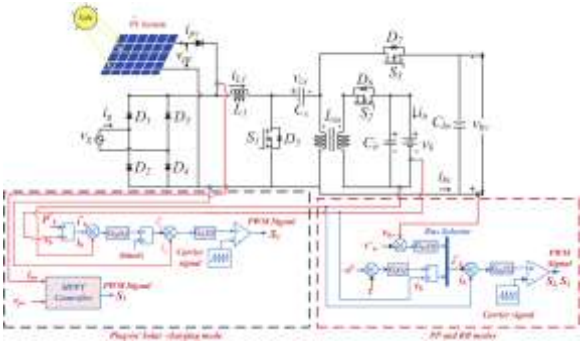

Fig. 7 Control structure of a proposed system

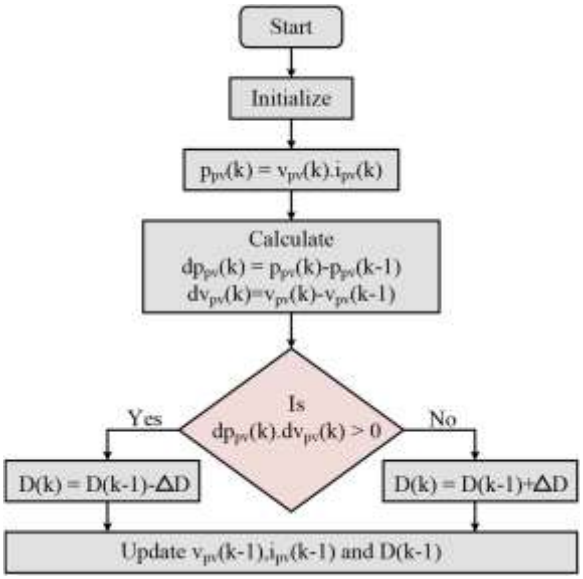

Fig. 8 Flowchart for MPPT operation

the reference and measured quantities is fed to the outer PI controller and generates reference charging power (Pb), which is then divided by instantaneous battery voltage (vb) to generate a reference signal for the inner PI controller. The parameters of each PI controller are set through trial and error based tuning method. 8 Results and discussions The simulation of the proposed converter has been verified in MATLAB/Simulink environment with grid voltage (Vg) is 220 V, battery nominal voltage (Vb) is 300 V, charging power is 1.2 kW and dc-link voltage (Vhv) is 400 V. Fig. 9 shows the waveforms of PIC mode. In this mode, the battery is charged through the grid and simultaneously converter operates in a PFC mode to wave-shape the grid current. In Fig. 9a, the grid voltage and current are in the same phase with sinusoidal shape, which shows the converter is operating in unity power factor (UPF) condition. The UPF operation of the converter is ensured by the closed-loop control system as discussed in the control section. The battery

voltage with 20% SOC and the battery current are shown in Figs. 9b and c, respectively.

From Fig. 9c, a low frequency oscillation (100 Hz) is observed in the battery current, which is inherent in the single-stage chargers, the maximum possible peak-to-peak battery current ripple will be twice of the average battery current. However, the low-frequency oscillation of battery current ripple can be suppressed by connecting an inductive filter in series with battery. However, addition and size of this filter

depend on battery types, cost and compactness of the charger. The measured grid RMS current and average battery current at 1.2 kW charging power are 5.8 and 3.90 A, respectively.

Table 5 shows the parameters of SPV system. The power versus voltage curve of a solar panel is shown in Fig. 10. The maximum power of PV panel is obtained around 800 and 400 W at 1000 and

500 W/m2 solar irradiation. The PV panel output at MPPT is shown in Fig. 11. The panel average output current is around 15 A and voltage at MPPT is 53 V. The battery is charged through the maximum power of PV, i.e. 800 W. During charging, the battery

voltage and battery current are shown in Figs. 12a and b, respectively. The measured battery current and battery voltage are around 2.45 A and 309 V and the calculate battery power is 757.05 W. Hence, the efficiency of the converter at 800 W charging power

is 94.6%.

In PP mode (driving operation), the battery supplies power to the dc-link capacitor for the acceleration of the vehicle. For smooth operation of vehicle, the dc-link voltage Vhv is kept constant. In the simulation study, the reference dc-link voltage is chosen as 400 V.

The dynamic operation of closed-loop control is tested with the step load changes, as shown in Fig. 13. At t = 1 s, load power is increased from 1 to 2 kW and again reduced to 1 kW at t = 2 s. The

load power further increases to 2 kW at t = 3 s. During these load changes, the dc-link voltage is regulated at 400 V, as shown in Fig. 13a and the corresponding changes in the battery voltage and current are shown in Figs. 13b and c, respectively. The measured battery current for 1 and 2 kW loads are around 3.4 and 6.9 A, respectively. Hence, calculated battery power are 1050.6 and

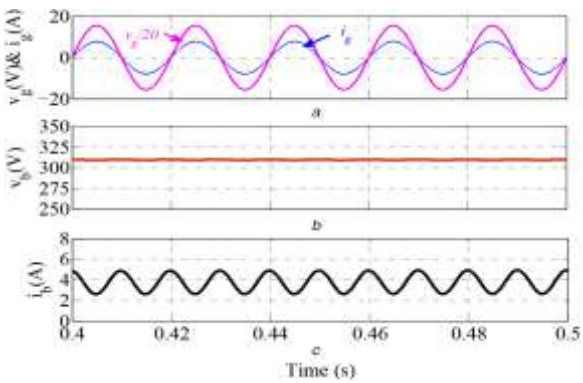

Fig. 9 Simulation results during PIC operation
(a) Grid voltage and grid current, (b) Battery voltage, (c) Battery current

Table 5 Characteristics of PV panel

Parameters of solar panel at nominal operating conditions	
maximum power current (I_{mp})	7.61 A
maximum power voltage (V_{mp})	26.3 V
maximum power (P_{max})	200.13
short-circuit current (I_{sc})	8.21 A
open-circuit voltage (V_{oc})	32.9 V
number of series cell in each module (N_s)	54
number of series and parallel connected module (N_{sp},N_{pp})	2, 2

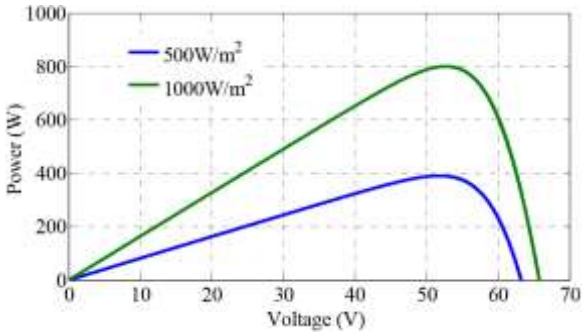

Fig. 10 Simulation result of PV panel at 500 and 1000 W/m2 irradiations

2132.1 W. Therefore, the simulation efficiency of the converter at 1

and 2 kW 95.2 and 93.8%, respectively. In RB operation, the battery is charged with braking energy of the motor. The simulated wave forms of this mode are shown in Fig. 14. To verify this mode, the dc-link voltage is varied linearly from 250 to 325 V and kept constant at 325 V for t = 1.5 to 2 s then linearly reduced to 300 V, as shown in Fig. 14a, and the battery is charged with 3.5 A current, as shown in Fig. 14c. The duty signal variation with dc-link voltage is shown in Fig. 14d. When dc-link

voltage is higher than battery voltage, the converter operates in buck mode and duty signal is below 0.5. Moreover, when the dclink voltage falls below the battery voltage, the converter operates in boot mode and duty signal is above 0.5. A small-scale prototype model was built for the verification of the proposed work, which is depicted in Fig. 15. The battery voltage is 48 V and the dc-link voltage is 150 V. Fig. 16 shows the experimental waveforms during PIC mode. For 1 kW charging power and 110 V peak grid voltage (Vgmax), the waveforms of grid current (ig) and grid voltage (vg) are shown in Fig. 16 at CH1 and CH2, respectively. This figure shows that the ig and vg are in the same phase with sinusoidal shape, which indicates converter is operating near unity power factor (UPF) condition.

The UPF operation of the converter mitigates reactive power burden on the grid system and reduces the electricity usages from the grid. The battery charging from solar PV is

accomplished through rooftop panel. At the time of experimentation, the measured solar
irradiation was 620 W/m2 and available maximum power was around 480 W.

The battery voltage and battery current have been shown in Fig. 17. From this figure, measured battery current is around 9.27 A and calculated battery side power is 445 W. Hence, calculated experimental efficiency of the converter is 92.7%. The waveforms of PP mode with 150 V dc-link CH1 and 48 V battery CH2 are shown in Fig. 18a. The dynamic operation of this mode is tested with step load changes from 400 to 500 W and from 500 to 400 W and corresponding changes in the battery voltage and current are recorded at CH2 and CH3, respectively in Fig. 18b. The control target is to keep the dc-link voltage at 150 V with load

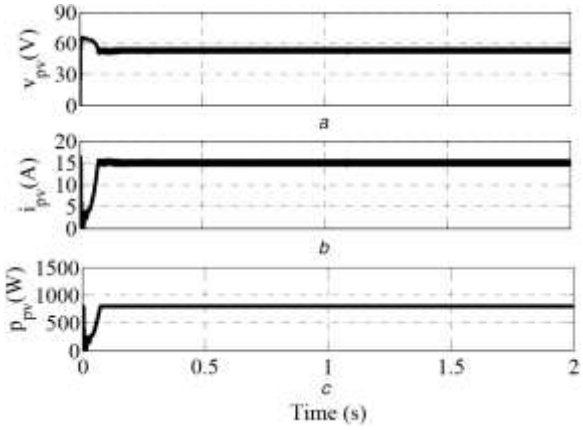

Fig. 11 SPV panel outputs (a) Panel output voltage, (b) Output current, (c) Output power

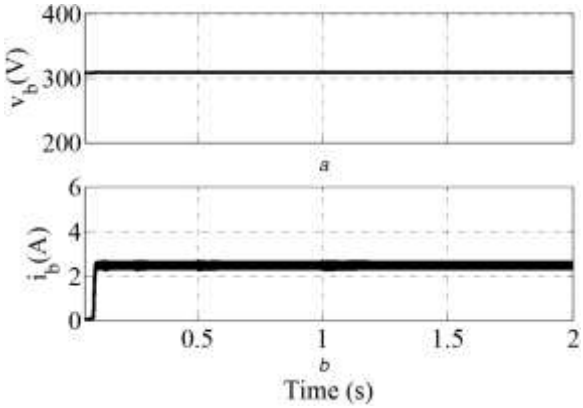

Fig. 12 Simulation results during battery charging from solar (a) Battery voltage, (b) Battery current

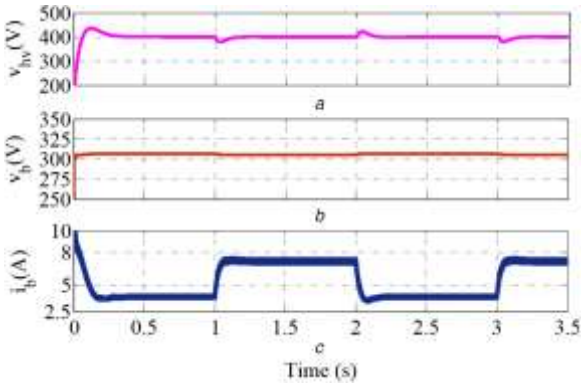

Fig. 13 Simulated waveforms during PP mode
(a) Dc-link voltage, (b) Battery voltage, (c) Battery current

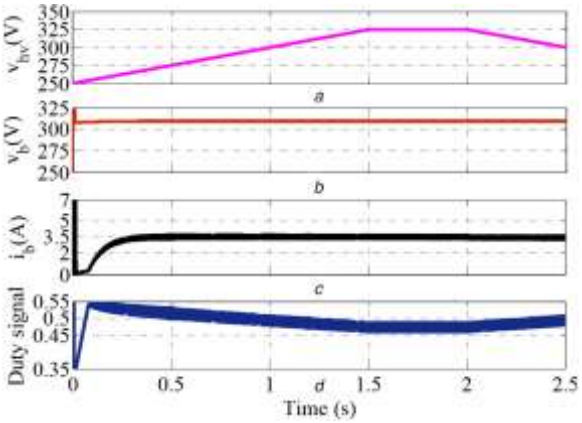

Fig. 14 Simulated waveforms during RB mode
(a) Dc-link voltage, (b) Battery voltage, (c) Battery current, (d) Duty signal

VI.CONCLUSION

In this paper, a compact multifunctional PEI has been proposed for the on-board applications of PEVs. The proposed PEI operates effectively in all vehicular modes. Reliability of the proposed converter is high due to dual sources for the battery charging, i.e. grid and SPV. This way, utilisation of fossil fuel-based electricity is reduced. The structure of the proposed PEI is designed to provide isolation in each mode, which results in higher safety of battery and vehicle users. Moreover, the proposed PEI performs buck/ boost operation effectively in all vehicular modes without any design modification. Because of this, the battery can be charged from any available charging point. This is significant for the evolution of EVs technology in the developing countries since dedicated EVs charging stations are currently unavailable. Compactness is accomplished by integrating the PV system through front-end charging converter; this eliminates the need of another dc/dc converter during charging operation for MPPT. The dynamic operation of the converter has been tested in
simulation and hardware for PP and RB modes to show theffectiveness of controller performance.10

References

[1] ‘SAE electric vehicle and plug-in hybrid electric vehicle conductive charge coupler’. SAE std. J1772, 2010
[2] Patil, D., Sinha, M., Agarwal, V.: ‘A cuk converter based bridgeless topology
for high power factor fast battery charger for electric vehicle application’. 2012 IEEE Transportation Electrification Conf. and Expo (ITEC), Dearborn, MI, USA, 2012, pp. 1–6

[3] Shi, L., Meintz, A., Ferdowsi, M.: 'Single-phase bidirectional AC-DC converters for plug-in hybrid electric vehicle applications'. 2008 IEEE Vehicle Power and Propulsion Conf., Harbin, China, 2008, pp. 1–5
[4] Yilmaz, M., Krein, P.T.: 'Review of battery charger topologies, charging power levels, and infrastructure for plug-in electric and hybrid vehicles', IEEE Trans. Power Electron., 2013, 28, (5), pp. 2151–2169
[5] Onar, O.C., Kobayashi, J., Erb, D.C., et al.: 'A bidirectional high-powerquality grid interface with a novel bidirectional noninverted buck–boost converter for PHEVs', IEEE Trans. Veh. Technol., 2012, 61, (5), pp. 2018– 2032
[6] Bendien, J.C., Fregien, G., van Wyk, J.D.: 'High-efficiency on-board battery charger with transformer isolation, sinusoidal input current and maximum
power factor', IEE Proc. B - Electr. Power Appl., 1986, 133, (4), pp. 197–204
[7] Singh, A.K., Pathak, M.K.: 'An improved two-stage non-isolated converter for on-board plug-in hybrid EV battery charger'. 2016 IEEE 1st Int. Conf. on Power Electronics, Intelligent Control and Energy Systems (ICPEICES), New Delhi, India, 2016, pp. 1–6
[8] Singh, A.K., Pathak, M.K.: 'Single-phase bidirectional ac/dc converter for plug-in electric vehicles with reduced conduction losses', IET Power
Electron., 2018, 11, (1), pp. 140–148
[9] Singh, A.K., Pathak, M.K.: 'Single-stage zeta-sepic-based multifunctional integrated converter for plug-in electric vehicles', IET Electr. Syst. Trans.,
2018, 8, (2), pp. 101–111
[10] Singh, A.K., Pathak, M.K.: 'A multi-functional single-stage power electronic interface for plug-in electric vehicles application', Electr. Power Compon.
Syst., 2018, 46, (2), pp. 135–148
[11] Chinmaya, K.A., Singh, G.K.: 'Integrated onboard single-stage battery charger for PEVs incorporating asymmetrical six-phase induction machine', IET Electr. Syst. Trans., 2019, 9, (1), pp. 8–15
[12] Lee, Y.J., Khaligh, A., Emadi, A.: 'Advanced integrated bidirectional AC/DC and DC/DC converter for plug-in hybrid electric vehicles', IEEE Trans. Veh. Technol., 2009, 58, (8), pp. 3970–3980
[13] Rippel, W.E., Cocconi, A.G., assignees: 'Integrated motor drive and recharge system'. 5 099 186, 1992
[14] Rippel, W.E., assignee: 'Integrated traction inverter and battery charger apparatus'. 4 920 475, 1990
[15] 'Combined electric device for powering and charging'. WO 2010/057892 A1, 2010
[16] Subotic, I., Bodo, N., Levi, E.: 'An EV drive-train with integrated fast charging capability', IEEE Trans. Power Electron., 2016, 31, (2), pp. 1461– 1471
[17] Subotic, I., Bodo, N., Levi, E., et al.: 'Isolated chargers for EVs incorporating six-phase machines', IEEE Trans. Ind. Electron., 2016, 63, (1), pp. 653–664
[18] Subotic, I., Bodo, N., Levi, E.: 'Single-phase on-board integrated battery chargers for EVs based on multiphase machines', IEEE Trans. Power Electron., 2016, 31, (9), pp. 6511–6523
[19] Biswas, S., Huang, L., Vaidya, V., et al.: 'Universal current-mode control schemes to charge li-ion batteries under dc/pv source', IEEE Trans. Circuits Syst. I, Regul.Pap., 2016, 63, (9), pp. 1531–1542
[20] Traube, J., Lu, F., Maksimovic, D., et al.: 'Mitigation of solar irradiance intermittency in photovoltaic power systems with integrated electric-vehicle charging functionality', IEEE Trans. Power Electron., 2013, 28, (6), pp. 3058–3067

Author1

Name: Mr. Pradip Ramdas Jadhav

Mr. Pradip Ramdas Jadhav is pursuing M. TECH degree in the stream of Electrical Power System from Matsyodari Shikshan Sanstha's College of Engineering and Technology, Jalna, DBATU University, Lonere. He has completed B. E. in the stream of Electrical Engineering from G. H. Raisoni Institute of Engineering & Technology, Pune

Author2:

Prof Mr. K Chandra Obula Reddy received Mtech in Power Electronics from the oxford college of engineering, Bangalore, VTU University, Belgaum. B.Tech in Electrical and Electronics Engineering from SVCET, chitoor, JNTU university Anantapur,A.P. He is currently

working as HOD and Professor in Department of Electrical Engineering at MSS's College of Engineering and Technology, Jalna

ACKNOWLEDGMENT

I am greatly obligated forever to my guide and HOD K .Chandra Obula Reddy and to all teaching and non-teaching staff who supported me directly and indirectly to complete my work. I am sincerely thankful to my principal Dr.S.K Biradar for their continued encouragement and active interest in my progress throughout the work I am grateful to be an M.Tech Electrical Power System student at Matsyodari Shikshan Sanstha 's College of Engineering and Technology, Jalna, Maharashtra